# Isoform diversity of the inositol trisphosphate receptor in cell types of mouse origin

Humbert De SMEDT*, Ludwig MISSIAEN, Jan B. PARYS, Robert H. HENNING, Ilse SIENAERT, Sara VANLINGEN, Antoon GIJSENS, Bernard HIMPENS and Rik CASTEELS

Laboratory of Physiology, Campus Gasthuisberg O/N, K.U. Leuven, B-3000 Leuven, Belgium

Previous reports suggested the expression of four or five different Ins(1,4,5)$P_3$ receptor [Ins(1,4,5)$P_3$R] isoforms in mouse cells [Ross, Danoff, Schell, Snyder and Ullrich (1992) Proc. Natl. Acad. Sci. U.S.A. **89**, 4265–4269; De Smedt, Missiaen, Parys, Bootman, Mertens, Van Den Bosch and Casteels (1994) J. Biol. Chem. **269**, 21691–21698]. To explore this diversity further, we have isolated and sequenced partial clones of two Ins(1,4,5)$P_3$R mRNAs from the mouse embryonic $C_3H10T_{\frac{1}{2}}$ cell line. These clones showed between 94.2 and 94.9% sequence identity with the corresponding rat Ins(1,4,5)$P_3$R-II and Ins(1,4,5)$P_3$R-III isoforms. Based on these newly obtained sequences we have determined the relative expression of the different Ins(1,4,5)$P_3$R mRNAs in cultured cells and in animal tissues of mouse origin by a ratio reverse transcriptase polymerase chain reaction (RT-PCR). Ins(1,4,5)$P_3$R-I was very prominent in brain and cerebellum and Ins(1,4,5)$P_3$R-II in epithelia such as kidney as well as in both cardiac and skeletal muscle. Ins(1,4,5)$P_3$R-III was highly expressed in all cultured cell types and in tissues with high cell turnover, e.g. testis. The prominent expression of Ins(1,4,5)$P_3$R-I and Ins(1,4,5)$P_3$R-III in A7r5 and $C_3H10T_{\frac{1}{2}}$ cells respectively was confirmed by immunoblot analysis and was compatible with a lower threshold for Ins(1,4,5)$P_3$-induced $Ca^{2+}$ release in the former cell type. Screening of a large number of mouse cell lines and tissues revealed the presence of Ins(1,4,5)$P_3$R-I as well as of the Ins(1,4,5)$P_3$R-II and Ins(1,4,5)$P_3$R-III isoforms which were identified in the present study, but in contrast with previous reports there was no evidence for more isoform diversity.

## INTRODUCTION

Intracellular $Ca^{2+}$ channels release $Ca^{2+}$ from intracellular stores upon activation by a broad range of extracellular stimuli [1,2]. These channels have been increasingly characterized at the molecular level and were found to include the inositol 1,4,5-trisphosphate receptor [Ins(1,4,5)$P_3$R] and ryanodine receptor gene families, which both consist of at least three distinct members in mammalian cell types [3]. We have previously described a ratio reverse transcriptase polymerase chain reaction (RT-PCR) method which allows the quantitative determination of the relative amounts of the related mRNAs of different Ins(1,4,5)$P_3$R isoforms [4]. The method was based on the principles of competitive PCR, and consisted of the amplification of a small part of the mRNAs in a region of very high similarity. The primer pairs were chosen to be identical for two or more mRNAs, and discrimination of the amplification products was based on isoform-specific restriction analysis. The distribution of the different Ins(1,4,5)$P_3$R mRNAs showed a cell-type specific pattern. Some of these data were confirmed by RNA blot analysis [5]. There was also a good agreement with a determination of the relative expression at the protein level using isoform-specific antibodies [6]. The latter finding gave support to the assumption that the pattern obtained by the RT-PCR screening reliably reflects the relative expression of the different Ins(1,4,5)$P_3$Rs. The ratio RT-PCR method yielded reliable results, at least for rat mRNAs, for which complete sequence information was available [7–9]. Recently we have also determined the Ins(1,4,5)$P_3$R expression patterns in samples from human origin, using the same technique [10]. Also in the latter case, full sequence information for the different mRNAs was available [11–14].

For samples from mouse cell types, however, we have obtained a very limited expression pattern [4]. We could detect the mouse isoform of Ins(1,4,5)$P_3$R-I, but none of the other isoforms (II, III, and IV) for which partial and very limited sequence information is available [15], could be detected. Instead we have found and partially cloned a new mRNA which only slightly deviated from the published type II and type IV isoforms, and which we have tentatively designated as type V [4]. On the other hand we could find no detectable levels of a type III mRNA in mouse samples, although the presence of Ins(1,4,5)$P_3$R-III in cell types from mouse origin was evident from RNA blot analysis [5] and from hybridization analysis *in situ* [16].

In order to explain these controversies we have now partially cloned and sequenced the type II and type III Ins(1,4,5)$P_3$R present in mouse $C_3H10T_{\frac{1}{2}}$ fibroblasts. The clone representing part of Ins(1,4,5)$P_3$R-II was 3237 nt long and included the entire sequence of the PCR clone that we previously designated as Ins(1,4,5)$P_3$R-V [4]. A clone representing 639 nt of Ins(1,4,5)$P_3$R-III was RT-PCR amplified from $C_3H10T_{\frac{1}{2}}$ cell mRNA. The clones for type II and type III Ins(1,4,5)$P_3$Rs obtained in our study showed approx. 94.5% identity with the corresponding sequences from the rat Ins(1,4,5)$P_3$Rs. Moreover these clones deviated to exactly the same extent from the previously reported partial sequences for mouse type II and III Ins(1,4,5)$P_3$R isoforms [15]. We have then developed a ratio RT-PCR method based on the newly cloned sequences. In this way we obtained a consistent and reliable amplification of the mouse analogues of three types of Ins(1,4,5)$P_3$R mRNAs, and we could quantify their relative

Abbreviations used: Ins(1,4,5)$P_3$R, Ins(1,4,5)$P_3$ receptor; RT-PCR, reverse transcriptase polymerase chain reaction; FCS, fetal-calf serum; DMEM, Dulbecco's modified Eagle's medium; 3′UTR, 3′untranslated region; CHO, Chinese-hamster ovary.

* To whom correspondence should be addressed.

The nucleotide sequences reported in this paper have been submitted to the EMBL data bank with accession numbers Z71173 and Z71174.

expression levels in a number of mouse cell types from cell culture as well as from animal tissues. We could not, however, detect amplification products corresponding to the previously published type II, III or IV sequences [15] in any of the investigated mouse cell types. It is conceivable that the latter isoforms were erroneously described as mouse sequences. In view of their high degree of similarity to rat Ins(1,4,5)$P_3$ receptors, we believe that they rather represent sequences from rat or a very related species.

## EXPERIMENTAL PROCEDURES

### Cells and tissues

$C_3H10T_{\frac{1}{2}}$ mouse embryonic fibroblasts (ATCC CCL 226), L cells from mouse connective tissue (ATCC CCL 1), Swiss 3T3 embryonic mouse fibroblasts (ATCC CCL 92) and A7r5 smooth-muscle cells (ATCC CRL 1444) were cultured in Dulbecco's modified Eagle's medium (DMEM) supplemented with 10% fetal-calf serum (FCS) as described previously [17]. $BC_3H1$ mouse embryonic myoblasts (ATCC CRL 1443) and Sol8 myoblasts (kindly provided by Dr. C. Pinset, Institut Pasteur, CNRS, Paris, France) were cultured in the same medium but with 20% FCS. C2C12 myoblasts (ATCC CRL 1772) were cultured in 10% FCS and 0.5% chick-embryo extract. Differentiation of the muscle cells was induced by switching to a differentiation medium with 0.5% FCS for $BC_3H1$ and for Sol8 cells, or with 1% horse serum and 0.5% of a medium supplement consisting of insulin, transferrin and selenite (Sigma–Aldrich, Belgium) for C2C12 cells. The cells were allowed to differentiate during 6 days. Neuro-2a neuroblastoma cells (ATCC CCL 131) were cultured in DMEM/Ham's F12 medium with 10% FCS. To induce neurite outgrowth, cells were plated at a $1.8 \times 10^4/cm^2$ cell density, and 48 h after plating, FCS in the medium was reduced to 2% while 20 $\mu$M retinoic acid was added for an additional period of 48 h [18]. Tissues were dissected from adult male NMRI mice which were sacrificed after anaesthetizing with diethyl ether. The tissues were minced and immediately frozen in liquid nitrogen and stored at −80 °C until use.

### Cloning and sequencing

An oligo(dT)-primed cDNA library from $C_3H10T_{\frac{1}{2}}$ cells was prepared using the ZAP-cDNA® Synthesis Kit (Stratagene). The double-stranded cDNAs were unidirectionally ligated into the $\lambda$ZAP-II vector and packaged using the Gigapack® II Gold Packaging Extract (Stratagene). The cDNA library was screened with a random-primed PCR-generated cDNA probe corresponding to nt 203–1061 of type II-like Ins(1,4,5)$P_3$R mRNA (EMBL: Z33908) that was previously detected and PCR-amplified from $C_3H10T_{\frac{1}{2}}$ cells [4]. Positive clones were plaque-purified and Bluescript pB SK(−) phagemids were excised according to the manufacturer's instructions. Six different clones were sequenced, including the longest clone which contained 3237 nt of the 3′ end of the type II Ins(1,4,5)$P_3$R from $C_3H10T_{\frac{1}{2}}$ cells. A 639 nt cDNA clone representing the type III Ins(1,4,5)$P_3$R in these cells was RT-PCR-amplified from reverse-transcribed $C_3H10T_{\frac{1}{2}}$ total RNA, using a forward (agtggggacaagatggactgtgtc; nt 7407–7430) and a reverse (gtgcgagaccagcttcatggtgg; nt 8023–8045) primer based on a consensus domain in both the rat [9] and human [12] type III Ins(1,4,5)$P_3$Rs. The nt values refer to the positions in the rat sequence.

Nucleotide sequencing of the different clones was performed in both directions by means of dideoxy sequencing using an A. L. F. sequenator (Pharmacia–LKB). The sequence of the previously published PCR-amplified type II-like Ins(1,4,5)$P_3$R from $C_3H10T_{\frac{1}{2}}$ cells [4] is identical with and entirely contained within the present sequence which was derived from the cDNA library.


**Figure 1 Location of the RT-PCR primer pairs on the sequences of the different mouse Ins(1,4,5)$P_3$R isoforms**

Only the relevant part of the sequences is shown. The co-ordinates refer to the published sequence of Ins(1,4,5)$P_3$R-I [20] and of the clones for type II (accession number: Z71173) and type III (accession number: Z71174) Ins(1,4,5)$P_3$Rs obtained in the present study. The positions of the forward and reverse primer pairs are indicated: underlined, Ins(1,4,5)$P_3$R-I/Ins(1,4,5)$P_3$R-II ratio; bold underlined, Ins(1,4,5)$P_3$R-I/Ins(1,4,5)$P_3$R-III ratio; broken underlined, Ins(1,4,5)$P_3$R-II/Ins(1,4,5)$P_3$R-III ratio. Conserved bases are indicated by asterisks. Diverging bases within a particular primer pair were always at least 12 nucleotides removed from the 3′ end of the primer. In such case a mixture of primers was used.

### RNA preparation and ratio RT-PCR analysis

For the cultured cells total RNA was prepared according to [19]. For the tissues we have isolated poly(A)$^+$ RNA using the Micro-Fast Track™ kit (Invitrogen). Random-primed first-strand cDNA was synthesized using avian myeloblastosis virus reverse transcriptase (Boehringer-Mannheim Belgium). The ratio RT-PCR assay used in the present study was based on the simultaneous amplification of two or more targets which had identical primer template sequences. The amplified products were discriminated using restriction enzymes with a specific cleavage site in the diverging areas of the targets. The primers

**Table 1 Isoform-specific restriction-enzyme digestion of the ratio PCR products for the mouse $InsP_3R$ isoforms**

The restriction analysis was done for the three different PCR products representing the three mouse $InsP_3R$ isoforms described in the present study. The length and the CG content of the fragments is given in nt units. I, II and III refer to fragments from $InsP_3R$ type I, II and III respectively.

| $InsP_3R$-I/$InsP_3R$-II primer pair (215 nt fragment) | | | | $InsP_3R$-I/$InsP_3R$-III primer pair (294 nt fragment) | | | | $InsP_3R$-II/$InsP_3R$-III primer pair (281 nt fragment) | | | |
|---|---|---|---|---|---|---|---|---|---|---|---|
| Enzyme | Fragment | Length (nt) | C + G (nt) | Enzyme | Fragment | Length (nt) | C + G (nt) | Enzyme | Fragment | Length (nt) | C + G (nt) |
| *Bgl*II | Ia | 107 | 52 | *Bgl*II | Ia | 53 | 26 | *Bgl*II | Ia | 190 | 91 |
| | Ib | 108 | 47 | | Ib | 241 | 116 | | Ib | 91 | 44 |
| *Asp*I | IIa | 168 | 74 | *Asp*I | IIa | 114 | 50 | *Asp*I | IIa | 152 | 66 |
| | IIb | 47 | 23 | | IIb | 180 | 93 | | IIb | 129 | 67 |
| | IIIa | 168 | 79 | | IIIa | 114 | 56 | | IIIa | 152 | 72 |
| | IIIb | 47 | 22 | | IIIb | 180 | 95 | | IIIb | 129 | 64 |
| *Bst*NI | IIa | 139 | 63 | *Eco*NI | IIa | 181 | 83 | *Bst*NI | IIa | 65 | 36 |
| | IIb | 76 | 32 | | IIb | 113 | 60 | | IIb | 93 | 42 |
| | | | | | | | | | IIc | 123 | 55 |
| *Taq*I | Ia | 62 | 29 | *Pml*I | Ia | 68 | 31 | *Taq*I | Ia | 235 | 114 |
| | Ib | 153 | 70 | | Ib | 226 | 111 | | Ib | 46 | 21 |
| | IIIa | 62 | 26 | | IIIa | 68 | 34 | | IIIa | 121 | 60 |
| | IIIb | 114 | 57 | | IIIb | 226 | 117 | | IIIb | 114 | 57 |
| | IIIc | 39 | 18 | | | | | | IIIc | 46 | 19 |
| *Hin*PI | IIIa | 81 | 37 | *Afl*II | IIIa | 58 | 30 | *Hin*PI | IIIa | 65 | 30 |
| | IIIb | 134 | 64 | | IIIb | 236 | 121 | | IIb | 216 | 106 |
| *Dde*I | Ia | 79 | 39 | *Hph*I | Ia | 108 | 50 | *Bss*KI | Ia | 246 | 114 |
| | Ib | 136 | 60 | | Ib | 84 | 38 | | Ib | 35 | 21 |
| | IIa | 79 | 34 | | Ic | 102 | 54 | | IIa | 67 | 38 |
| | IIb | 136 | 63 | | IIa | 192 | 88 | | IIb | 93 | 42 |
| | | | | | IIb | 6 | 5 | | IIc | 121 | 53 |
| | | | | | IIc | 96 | 50 | | | | |

used were based on the published sequence for Ins(1,4,5)$P_3$R-I [20] and on the sequences for the type II and type III Ins(1,4,5)$P_3$Rs, which were derived from $C_3H10T\frac{1}{2}$ clones obtained in the present study. An overview of these primers and their co-ordinates with respect to the mouse Ins(1,4,5)$P_3$R-I [20], and the mouse type II and type III Ins(1,4,5)$P_3$Rs cloned in the present study, is given in Figure 1. Three different primer pairs were used. As can be expected from the data in Figure 1, each primer pair allowed an optimal amplification of two isoforms and no or very little amplification (the latter was the case for the primer pair designed for optimal amplification of the type II and type III isoforms) of the remaining isoform. In order to obtain a perfect match with the mRNAs for which an optimal amplification with identical efficiency was required, mixtures of primers were used. The diverging nucleotide was always located as far as possible from the primer's 3′-end, and whenever possible it represented a change to the complementary base (Figure 1). The amplification reaction mixture (50 $\mu$l) contained 0.4–2 % of the first-strand reaction product and in addition 10 nmol of each dNTP, 25 pmol of the 5′ and 3′ primers, and 2.5 units of AmpliTaq® DNA polymerase (Perkin–Elmer Belgium) in the supplied buffer supplemented with 1 mM $Mg^{2+}$. The protocol included a first cycle consisting of 3 min of denaturation at 94 °C, 1 min annealing at 54 °C 52.5 °C or 55 °C for the first, second and third primer pair respectively, and 2 min extension at 72 °C, followed by 25–26 cycles consisting of the same steps but with only 1 min of denaturation. Radioactive labelling was done by a 20-fold dilution of the reaction product in the complete RT-PCR mixture supplemented with 10 nCi/$\mu$l [$\alpha$-$^{32}$P]dCTP (Amersham International) for three to five additional cycles. Evaluation of the expression of the different mRNAs was done by digestion with restriction enzymes as described elsewhere [4]. An overview of the restriction enzyme analysis for isoform-specific digestion of the RT-PCR products representing either one or two of the mouse Ins(1,4,5)$P_3$R isoforms is shown in Table 1.

## Microsome preparations and protein analysis

Microsomes of rabbit cerebellum, A7r5 smooth-muscle cells and $C_3H10T\frac{1}{2}$ fibroblasts were prepared as described [21]. Microsomes from undifferentiated $BC_3H1$ cells were prepared similarly, except that an additional centrifugation step (10 min, 10000 ***g***) was included. Protein determination was according to Lowry et al. [22]. Proteins were separated by SDS/PAGE [23] on 3–12 % linear gradient gels and analysed by Western blotting after transfer to Immobilon P [21]. Rbt04, an isoform-specific antibody against Ins(1,4,5)$P_3$R-I, and Rbt02, an isoform-specific antibody against Ins(1,4,5)$P_3$R-II, were previously described [21]. A monoclonal antibody against Ins(1,4,5)$P_3$R-III was obtained from Transduction Laboratories (Lexington, KY, U.S.A.). Appropriate controls were performed to assure that neither of the antibodies cross-reacted.

## $^{45}Ca^{2+}$-flux experiments

$C_3H10T\frac{1}{2}$ cells were seeded in 4 $cm^2$ gelatin-coated 12-well clusters (Costar) at a density of approx. $10^4$ cells/$cm^2$. A7r5 cells were seeded at a similar density in non-coated 12-well clusters. Experiments were carried out with confluent monolayers of cells on the 5th or 6th day after plating. $^{45}Ca^{2+}$ fluxes on permeabilized cells were done on a thermostatically controlled plate at 25 °C. The culture medium was aspirated and replaced by 1 ml permeabilization medium [120 mM KCl/30 mM imidazole/HCl (pH 6.8)/2 mM $MgCl_2$/1 mM ATP/1 mM EGTA/saponin

(20 $\mu$g/ml)]. The saponin-containing solution was removed after 10 min and the cells were washed once with a similar saponin-free solution. $^{45}Ca^{2+}$ uptake into the non-mitochondrial $Ca^{2+}$ stores was accomplished by incubation for 60 min in 2 ml of loading medium containing 120 mM KCl/30 mM imidazole/HCl, pH 6.8/5 mM $MgCl_2$/5 mM ATP/0.44 mM EGTA/10 mM $NaN_3$/100 nM free $^{45}Ca^{2+}$. After this phase of $^{45}Ca^{2+}$ accumulation, the monolayers were incubated in 1 ml of efflux medium [120 mM KCl/30 mM imidazole/HCl (pH 6.8)/2 mM $MgCl_2$/1 mM ATP/1 mM EGTA/100 nM free $^{45}Ca^{2+}$/2 $\mu$M thapsigargin]. Ins(1,4,5)$P_3$ was added as indicated in Figure 5. The first 5 min of efflux were not monitored. From 5 min onwards, the efflux medium was collected every 6 s. At the end of the experiment the $^{45}Ca^{2+}$ remaining in the stores was released by incubation with 1 ml of a 2% SDS solution for 30 min.

## RESULTS

### Ins(1,4,5)$P_3$R isoforms in $C_3H10T_{\frac{1}{2}}$ cells

In a previous study we have PCR-amplified an Ins(1,4,5)$P_3$R mRNA which was present in different cell lines from mouse origin and was particularly prominent in $C_3H10T_{\frac{1}{2}}$ cells [4]. The sequence, however, slightly deviated from the published mouse isoforms of type II, III and IV, which were obtained from a mouse placenta cDNA library [15]. We therefore designated the $C_3H10T_{\frac{1}{2}}$ cell isoform as a new type [Ins(1,4,5)$P_3$R-V]. This type V Ins(1,4,5)$P_3$R showed much larger similarity to type II or type IV sequences than to type III or type I sequences. We wanted to investigate whether the type II Ins(1,4,5)$P_3$R could be represented by a family of several very related members and whether such isoforms were co-expressed in some cell types. We therefore screened a $C_3H10T_{\frac{1}{2}}$-cell cDNA library using a cDNA probe derived from the amplified type-V PCR product. Twenty-one positive clones were obtained, which were all overlapping and started from an A-rich region which was located 210 nt downstream of the beginning of the 3′ untranslated region (3′-UTR). This region corresponds to a similar region at nt 8543–8559 in the 3′UTR of the rat $IP_3$R-II about 2140 nt from the end of the mRNA. Six of these clones were sequenced and the others were characterized by restriction-enzyme analysis. It became evident that all clones represented the same mRNA, which was identical with the previously found type V Ins(1,4,5)$P_3$R.

Since there were very good indications at the mRNA level [5], as well as from antibody data (see below) that a type III Ins(1,4,5)$P_3$R was present in some of the investigated mouse cell lines, including $C_3H10T_{\frac{1}{2}}$ cells, we attempted to amplify the corresponding mRNA by RT-PCR. We used primers in a region of very high homology, i.e. where the human and the rat Ins(1,4,5)$P_3$R-III sequences matched perfectly. The 639 nt sequence thus obtained was clearly representative of a type III mRNA but again it slightly deviated from the previously published mouse Ins(1,4,5)$P_3$R-III sequence [15].

A comparison of the available sequence data with sequences for rat Ins(1,4,5)$P_3$Rs is presented in Table 2. There was, depending on the length of the fragment, between 94.3% and 94.9% identity between the rat Ins(1,4,5)$P_3$Rs and the mouse isoforms obtained in our study. This identity is exactly what was expected considering the identity (in %) between rat and mouse Ins(1,4,5)$P_3$R-I, for which full sequence information is available. Based on this degree of sequence identity, one can conclude that the clones derived here from $C_3H10T_{\frac{1}{2}}$ cells represent the mouse analogues of the fully cloned rat Ins(1,4,5)$P_3$Rs. The sequences derived from the mouse placenta library [15], however, show much more identity with rat sequences (> 98%), and in fact deviate to the same extent from the sequences obtained in our study as do the rat sequences. In principle the observed differences could mean that there are as many as six different Ins(1,4,5)$P_3$R isoforms. It is very remarkable, however, that we could never detect any of the previously described sequences (type II, III or IV from [15]) in any of the investigated cell types or tissues of mouse origin, whereas the mRNAs described in the present study were clearly detected in all investigated cell types [4] (Table 3).

### RT-PCR analysis of the relative amounts of the three Ins(1,4,5)$P_3$Rs

We have therefore reinvestigated a number of mouse cell lines as well as tissues, using primer pairs designed to match with the mouse sequences obtained from $C_3H10T_{\frac{1}{2}}$ cells in the present study. As indicated in Figure 1, it was not possible to find a

**Table 2 Comparison of the nucleotide sequence identity between mouse and rat Ins$P_3$R isoforms**

Alignments were done using the method of Myers and Miller (PC/GENE, Intelligenetics, release 6.80). The positions indicated refer to the original sequence data: [a]MMP400 [20]; [b]MMIP3R2 and MMIP3R3, the present paper; [c]MMINSTPA, MMINSTPB, MMINSTPC [15]; [d]RRI145TR, [7]; [e]RNITPR2R [8]; [f]RATIP3R3X [9].

| | | | | Identity (% of the compared nucleotides) | | | | | |
|---|---|---|---|---|---|---|---|---|---|
| | Position (nt) | Length (nt) | $InsP_3R$ isoform … (organism) … | I (mouse)[a] | II (mouse)[b] | III (mouse)[b] | I (rat)[d] | II (rat)[e] | III (rat)[f] |
| I (mouse)[a] | 1–9848 | 9848 | | | | | 94.65 | | |
| II | 1–3237 | 3237 | | 63.63 | | | | 94.37 | |
| (mouse)[b] | 1419–3237 | 1819 | | | | | | 94.77 | |
| | 2371–2778 | 408 | | | | | | 94.36 | |
| III | 1–639 | 639 | | 71.36 | 73.08 | | | | 94.91 |
| (mouse)[b] | 1–555 | 555 | | | | | | | 94.23 |
| II[c] | 1–2333 | 2333 | | | | | | 98.07 | |
| | 1–1819 | 1819 | | | 94.34 | | | 99.17 | |
| III[c] | 1–613 | 613 | | | | | | | 96.08 |
| | 59–613 | 555 | | | | 92.25 | | | 98.01 |
| IV[c] | 131–538 | 408 | | | 94.61 | | | 99.26 | |

**Table 3 Expression levels of Ins$P_3$R isoforms in different mouse cell types**

The expression of Ins$P_3$R mRNAs was assayed in different cell lines and tissues from mouse origin as described in the Experimental procedures section. The values indicate the relative levels for the different Ins$P_3$R isoforms as % of the total. Values are means ± S.E. for three–six determinations.

| Cell type | Ins$P_3$R-I | Ins$P_3$R-II | Ins$P_3$R-III |
|---|---|---|---|
| $C_3H10T_{\frac{1}{2}}$ | 5.3 ± 0.4 | 20.4 ± 2.0 | 74.3 ± 2.2 |
| L cells | 11.7 ± 0.8 | 18.5 ± 2.6 | 69.8 ± 3.1 |
| Swiss 3T3 | 12.4 ± 0.8 | 9.3 ± 1.4 | 78.3 ± 1.9 |
| $BC_3H1$ (undifferentiated) | 12.5 ± 1.0 | 9.2 ± 0.6 | 78.3 ± 1.5 |
| $BC_3H1$ (differentiated) | 12.6 ± 0.9 | 12.1 ± 0.6 | 75.3 ± 1.2 |
| C2C12 (undifferentiated) | 5.2 ± 0.7 | 17.0 ± 0.7 | 77.8 ± 1.3 |
| C2C12 (differentiated) | 9.3 ± 1.1 | 27.9 ± 2.9 | 61.2 ± 4.1 |
| Sol8 (undifferentiated) | 10.5 ± 0.8 | 16.8 ± 1.7 | 71.6 ± 2.4 |
| Sol8 (differentiated) | 12.9 ± 1.0 | 24.2 ± 1.5 | 61.7 ± 2.0 |
| Neuro-2a (undifferentiated) | 33.3 ± 1.4 | 15.8 ± 0.9 | 50.5 ± 1.6 |
| Neuro-2a (differentiated) | 11.9 ± 1.0 | 30.0 ± 1.9 | 57.0 ± 2.3 |
| Cerebellum | 90.2 ± 1.7 | 4.1 ± 0.6 | 5.6 ± 1.2 |
| Brain | 68.8 ± 2.0 | 17.6 ± 1.4 | 13.6 ± 0.7 |
| Kidney | 43.3 ± 1.8 | 43.4 ± 1.8 | 13.3 ± 0.5 |
| Testis | 20.2 ± 1.1 | 25.4 ± 2.2 | 54.5 ± 2.3 |
| Thymus | 13.7 ± 0.8 | 40.8 ± 1.6 | 45.5 ± 1.4 |
| Pancreas | 18.5 ± 3.2 | 29.5 ± 3.6 | 52.1 ± 4.6 |
| Skeletal muscle | 16.3 ± 2.3 | 46.8 ± 3.1 | 36.9 ± 2.1 |
| Heart | 6.1 ± 0.6 | 78.0 ± 1.3 | 15.9 ± 2.4 |
| Liver | 3.6 ± 1.1 | 83.5 ± 19.0 | 12.8 ± 2.9 |

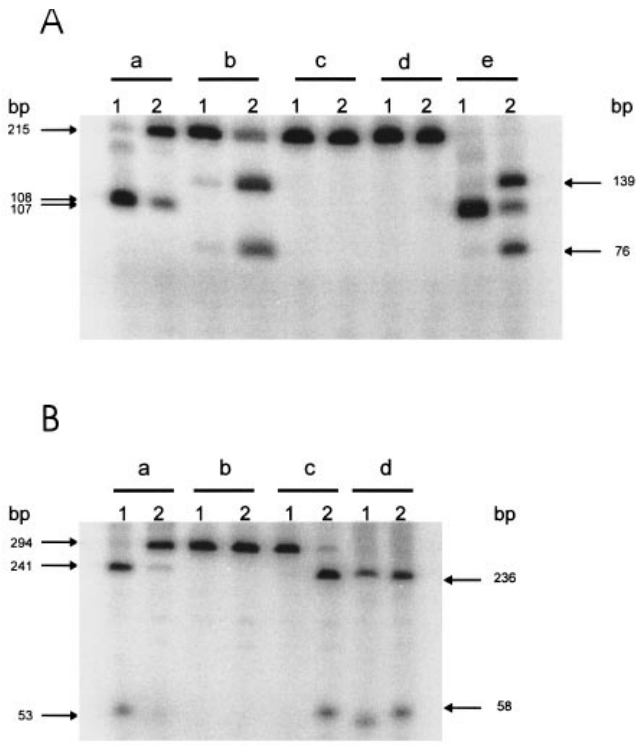


**Figure 2 Determination of the expression pattern of different Ins(1,4,5)$P_3$R isoforms in samples from mouse cerebellum and $C_3H10T_{\frac{1}{2}}$ cells**

Total RNA was reverse transcribed and RT-PCR-amplified as described in the Experimental procedures section. The sets of primers used for optimal amplification of either Ins(1,4,5)$P_3$R-I and Ins(1,4,5)$P_3$R-II (**A**), or Ins(1,4,5)$P_3$R-I and Ins(1,4,5)$P_3$R-III (**B**) are indicated in Figure 1. Two samples were compared: 1, mouse cerebellum; 2, $C_3H10T_{\frac{1}{2}}$ cells. The arrows indicate the length (in bp) of the PCR products and the restriction fragments for Ins(1,4,5)$P_3$R-I (left side) and for Ins(1,4,5)$P_3$R-II (**A**) or Ins(1,4,5)$P_3$R-III (**B**) on the right side. Lanes a and b represent a specific cut of Ins(1,4,5)$P_3$R-I by *Bgl*II and of Ins(1,4,5)$P_3$R-II by *Bst*NI respectively. Lanes c and d represent a similar analysis for Ins(1,4,5)$P_3$R-III using *Hin*PI and for the Ins(1,4,5)$P_3$R-IV sequence reported by Ross et al. [15] using Asp700 I. Lanes e represent a double digest using a combination of *Bgl*II and *Bst*NI. (**B**) represents a similar analysis for the primer pair designed for optimal amplification of Ins(1,4,5)$P_3$R-I and Ins(1,4,5)$P_3$R-III fragments. Lanes a–c represent a digestion using enzymes which are specific for Ins(1,4,5)$P_3$R-I (*Bgl*II), Ins(1,4,5)$P_3$R-II (*Eco*NI) and Ins(1,4,5)$P_3$R-III (*Afl*II) isoforms respectively. Lanes d represent a double digest using a combination of *Bgl*II and *Eco*NI.

primer pair that would match perfectly the sequences of all three isoforms. We have instead used three different primer pairs that could each amplify two out of three isoforms with optimal efficiency and have thus allowed us to determine the ratio of expression of these two isoforms. This analysis was first performed on mouse cerebellum and $C_3H10T_{\frac{1}{2}}$ samples. Figure 2(A) represents the results for the primer pair designed for the type I versus type II ratio determination. A PCR product of 215 nt was amplified. We have used *Bgl*II (lanes a), *Bst*NI (lanes b) and *Hin*PI (lanes c) restriction digestion in order to obtain a specific cut for type I, II and III Ins(1,4,5)$P_3$Rs respectively. As expected from the sequence data (Figure 1), this primer pair did not amplify Ins(1,4,5)$P_3$R-III (lanes c). Neither did Asp700 I (lanes d), which should digest the type IV Ins(1,4,5)$P_3$R according to its published sequence [15], affect the amplification product from these mouse samples, in agreement with our previous findings [4]. Ins(1,4,5)$P_3$R-I was the predominant amplification product for cerebellum, whereas the largest fraction of the amplification product from the $C_3H10T_{\frac{1}{2}}$ cell sample was represented by the type II mRNA. The lanes (e) in Figure 2(A) represent a control digestion showing that a combination of *Bgl*II and *Bst*NI could digest nearly all the PCR amplification product in these samples. A similar analysis was performed for the amplification product of 294 nt obtained using the primer pair designed for the analysis of the type I versus type III ratio (Figure 2B). In this case *Bgl*II, *Eco*NI and *Afl* II were used to digest type I, II and III respectively. It is again evident that Ins(1,4,5)$P_3$R-I is the prominent isoform in cerebellum, whereas type III is amplified to a much larger level than type I in $C_3H10T$ cells. As indicated in Table 1, the results were always complemented by digestion of all isoforms except one (specific leave). The results obtained by the latter type of digestion yielded essentially the same values for the respective isoforms (results not shown), and these values were also included in the final calculations.

Although the determination of the ratios type I/type II and type I/type III is sufficient for the calculation of the relative amounts of the three isoforms, we have also used a third primer pair in order to have an independent determination of the type II/type III ratio (Figures 3A and 3B). The lanes a represent the undigested amplification product of 281 nt. Lanes b, c and d show respectively a specific cut (*Bgl*II), a specific leave (*Asp*I) and a combination of both enzymes for Ins(1,4,5)$P_3$R-I. Although Ins(1,4,5)$P_3$R-I was present to a considerable extent in the cerebellum sample, this primer pair was expected to amplify type I only with low efficiency, and the results were therefore not used for determination of this mRNA. Lanes e, f and g represent a similar analysis for the type II Ins(1,4,5)$P_3$R with a specific cut by *Bst*NI, a specific leave by *Taq*I, and a combination of both. It is clear that a significant fraction of this amplification product in both samples is represented by the type II receptor. In Figure 3(B), lanes a, b and c represent the analysis for type III, with a specific cut by *Hin*PI, a specific leave by *Bss*KI and a combination of both. Both samples contained a type III product which is particularly prominent in $C_3H10T_{\frac{1}{2}}$ cells. From the combined analysis by the three primer pairs we calculated for cerebellum a

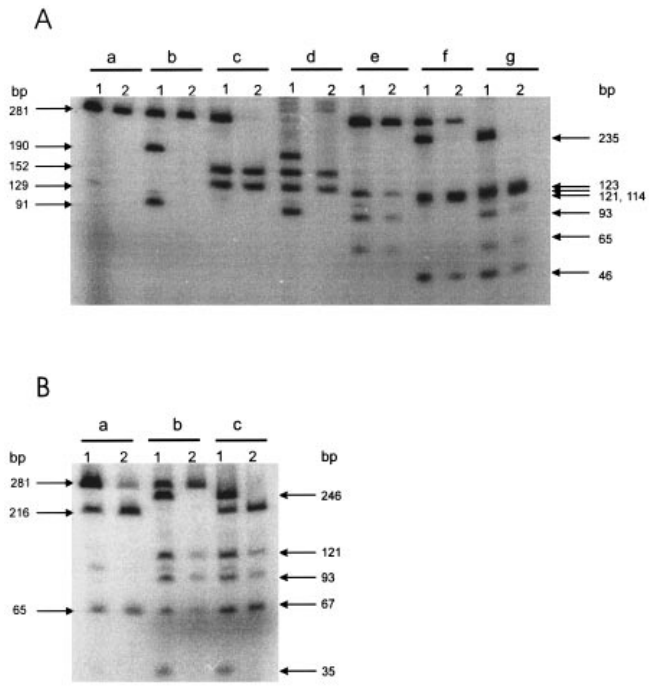


**Figure 3 Determination of the ratio of Ins(1,4,5)$P_3$R-II versus Ins(1,4,5)$P_3$R-III in mouse cerebellum and in $C_3H10T\frac{1}{2}$ cells**

The analysis was essentially done in the same way as described in Figure 2, but the primer pair designed to give an optimal amplification of Ins(1,4,5)$P_3$R-II and Ins(1,4,5)$P_3$R-III isoforms (Figure 1) was used. The same samples (1, mouse cerebellum; 2, $C_3H10T\frac{1}{2}$ cells) were used as described in Figure 2. The arrows indicate the length (in base pairs) of the PCR products and the restriction fragments for Ins(1,4,5)$P_3$R-I (left side) and for the other types (right side). (**A**) Lanes a–d (left arrows) represent the analysis for Ins(1,4,5)$P_3$R-I that was also amplified to some extent by this primer pair: a, undigested PCR product; b, *Bgl*II digestion producing a specific cut; c, Asp I producing digestion of all isoforms except type I; d, a total digestion by a combination of both enzymes. Lanes e–g (right arrows) represent the analysis for the type II isoform by *Bst*NI digestion producing a specific cut (lanes e), *Taq*I producing a specific leave with digestion of all isoforms except type II (lanes f), and a total digestion by combination of both enzymes (lanes g). (**B**) represents the analysis for Ins(1,4,5)$P_3$R-III using the same samples and the same primer pair as in (**A**). Lanes a show the digestion with *Hin*PI (left arrows) yielding a specific cut of type III, lanes b show digestion with *Bss*KI (right arrows) yielding a specific leave of type III and lanes c show a double digest with both enzymes.

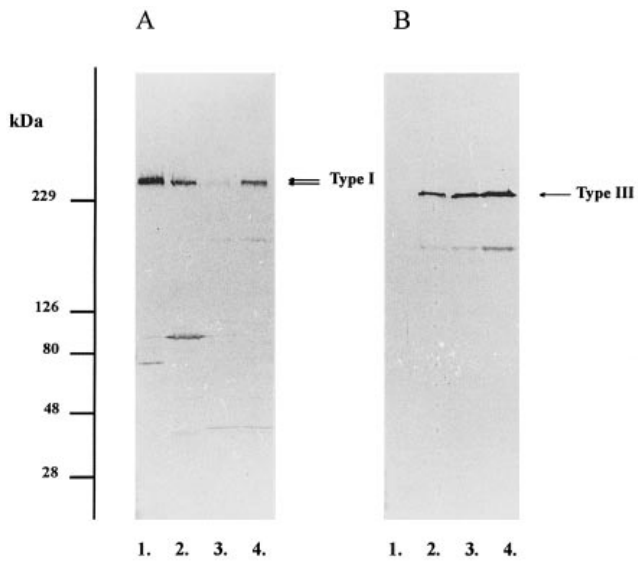


**Figure 4 Immunological detection of type I and type III Ins(1,4,5)$P_3$Rs**

Microsomes of cerebellum (lane 1, 25 $\mu$g), A7r5, $C_3H10T\frac{1}{2}$ and $BC_3H1$ cells (lanes 2–4, 200 $\mu$g) were separated by SDS/PAGE and transferred to Immobilon P. Analysis was performed with isoform-specific antibodies specifically reacting with Ins(1,4,5)$P_3$R-I (**A**) or with Ins(1,4,5)$P_3$R-III (**B**). Ins(1,4,5)$P_3$R-I migrates in neuronal samples (lane 1) with a molecular mass of 273 kDa (upper arrow), while in peripheral cell types (lanes 2–4) Ins(1,4,5)$P_3$R-I is characterized by a molecular mass of 261 kDa (lower arrow). The molecular masses of the standards are indicated on the left.

relative expression of Ins(1,4,5)$P_3$R-I/Ins(1,4,5)$P_3$R-II/Ins-(1,4,5)$P_3$R-III of 90:4:5 and for $C_3H10T\frac{1}{2}$ of 5:20:74 (Table 3). In contrast with our previous report, where we were unable to detect the type III receptor in $C_3H10T\frac{1}{2}$ cells, it now appears to be the most abundant isoform in these cells. Our failure to amplify the mouse Ins(1,4,5)$P_3$R-III in our previous study is due to the primers which we have used in that study. These primers were based on a published sequence for the mouse Ins(1,4,5)$P_3$R-III [15], which according to our present findings deviated by about 7% from the sequence of the mouse Ins(1,4,5)$P_3$R-III that is actually present in $C_3H10T\frac{1}{2}$ cells. This resulted in a deficient match for the selected PCR primers for Ins(1,4,5)$P_3$R-III in the previous study.

### Expression pattern of Ins(1,4,5)$P_3$R isoforms in different cell types

We then wanted to investigate whether the expression pattern obtained for $C_3H10T\frac{1}{2}$ cells was a typical property of these cultured cells and whether some tissue types would express other types of Ins(1,4,5)$P_3$R isoforms. We have therefore repeated the same type of analysis described above for a number of cell lines and a number of tissues of mouse origin. The results of this analysis are summarized in Table 3. It became clear that three different isoforms were co-expressed to some extent in all investigated cell types, although the level for every particular isoform may become very low in some cases. Ins(1,4,5)$P_3$R-I was, as expected, the main isoform in cerebellum and brain and was also very prominent in kidney. The type I isoform was relatively low, however, in the cultured cell types as well as in heart and skeletal muscle. Ins(1,4,5)$P_3$R-II, on the other hand, was relatively prominent in heart and skeletal muscle, in kidney and in the pancreas sample. The latter is in agreement with our previous finding for rat exocrine pancreas as well as for the AR42J pancreatic cell line [4]. Ins(1,4,5)$P_3$R-III was the major isoform expressed in all investigated cultured cell types. It is particularly striking that the presence of Ins(1,4,5)$P_3$R-III is much more pronounced in the cultured cells than in the samples obtained from different tissues. Among the tissue samples testis, thymus and pancreas also expressed type III as a major isoform.

### Detection of Ins(1,4,5)$P_3$R isoforms at the protein level

The presence of Ins(1,4,5)$P_3$R-III as a major isoform in many of the cultured cell lines was also confirmed at the protein level. In Figure 4 we show a Western-blot analysis on samples of rabbit cerebellum, A7r5 cells, $C_3H10T\frac{1}{2}$ cells and $BC_3H1$ cells. The Rbt04 antibody is directed against the C-terminus of the published mouse sequence of Ins(1,4,5)$P_3$R-I [20] and specifically recognizes the type I isoform in mouse, rat, rabbit and *Xenopus* [21], as well as in human and bovine cell types and tissues (J. B. Parys, unpublished work). Since Rbt04 displays such a broad spectrum of inter-species reactivity, we chose to use rabbit cerebellum and rat A7r5 cells as positive controls to facilitate comparisons with previous work [21,24,25]. The Ins(1,4,5)$P_3$R-I

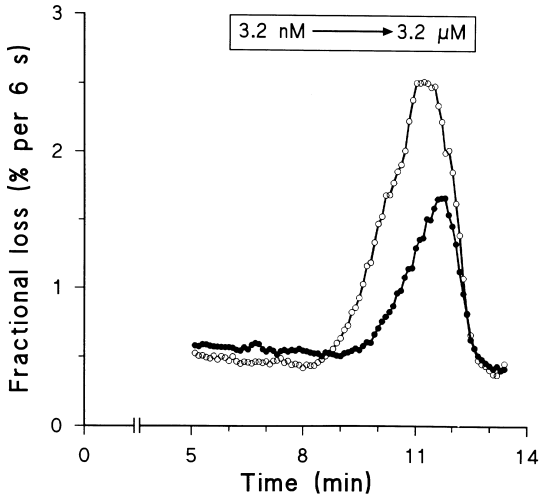


**Figure 5 Threshold for $Ca^{2+}$ release in A7r5 and $C_3H10T_{\frac{1}{2}}$ cells**

Stores of permeabilized A7r5 (○) and $C_3H10T_{\frac{1}{2}}$ cells (●) were loaded to steady state with $^{45}Ca^{2+}$, and from time 0 incubated in an unlabelled efflux medium containing 2 $\mu$M thapsigargin. The [Ins(1,4,5)$P_3$] was increased in an exponential way from 3.2 nM to 3.2 $\mu$M in 60 individual steps each lasting 6 s, as indicated by the bar above the traces. The results are plotted as fractional loss (the amount of $Ca^{2+}$ leaving the stores in 6 s divided by the total store $Ca^{2+}$ content at that time). Results are typical for three experiments.

isoforms detected in cerebellar or in whole brain tissues had a molecular mass of 273 kDa [21,24], which is significantly higher than the molecular mass of Ins(1,4,5)$P_3$R-I (261 kDa) of peripheral tissues [21]. This difference in molecular mass is unlikely to be due to differences in post-translational modifications, as for example glycosylation [24], but probably represents the expression of different splice isoforms [21]. As expected, the Rbt04 antibody recognized a 273 kDa protein in cerebellum (neuronal form) and a 261 kDa protein in the A7r5 cells (peripheral form) (Figure 4A, lanes 1 and 2 respectively). The latter protein was also detected in $C_3H10T_{\frac{1}{2}}$ and $BC_3H1$ cells, indicating the expression of type I receptors in those cell types (Figure 4A, lanes 3 and 4). The same samples were investigated for reactivity with a commercially available monoclonal antibody against the type III Ins(1,4,5)$P_3$R. At the indicated protein concentration, the antibody against Ins(1,4,5)$P_3$R-III gave no detectable response in the cerebellar microsomes, but it recognized a protein with a molecular mass of $248 \pm 2$ kDa ($n = 5$) in microsomes derived from A7r5, $C_3H10T_{\frac{1}{2}}$ and $BC_3H1$ cells (Figure 4B). The minor band at 177 kDa probably represents a proteolytic cleavage product. In addition, the anti-Ins(1,4,5)$P_3$R-III antibody also recognized the same protein in a number of cell lines of various origins, including RINm5F insulinoma cells, Chinese-hamster ovary (CHO) cells and HeLa cells (results not shown). The important point is that the Western-blotting experiments prove that mouse cell lines, like $C_3H10T_{\frac{1}{2}}$ and $BC_3H1$, where Ins(1,4,5)$P_3$R-III mRNA has previously gone undetected [4] express the type III Ins(1,4,5)$P_3$R not only at the mRNA level (Table 3) but also at the protein level. Moreover, comparison of the relative intensities of the staining by antibodies against type I or against type III respectively supports the mRNA data that Ins(1,4,5)$P_3$R-I is the predominant isoform in A7r5 cells [4], but that Ins(1,4,5)$P_3$R-III is predominant in $C_3H10T_{\frac{1}{2}}$ cells and in $BC_3H1$ cells (Table 3). We have previously demonstrated that $C_3H10T_{\frac{1}{2}}$ cells also expressed some Ins(1,4,5)$P_3$R-II at the protein level, but no type II Ins(1,4,5)$P_3$R was detected in brain nor in A7r5 samples [21]. In agreement with the mRNA data, we found in $BC_3H1$ cells only a very low expression of Ins(1,4,5)$P_3$R-II at the protein level (results not shown).

### Threshold for Ins(1,4,5)$P_3$-induced $Ca^{2+}$ release in A7r5 and $C_3H10T_{\frac{1}{2}}$ cells

A7r5 cells were characterized extensively with respect to their $Ca^{2+}$-release properties [26–29]. The expression pattern for Ins(1,4,5)$P_3$Rs in these cells is relatively simple, with type I as the major isoform (about 75 %), and a smaller amount (25 %) of the type III isoform. In Figure 5 we have compared the release properties of A7r5 cells with those of $C_3H10T_{\frac{1}{2}}$ cells where type III is the major isoform (74 %). Stores of permeabilized A7r5 and $C_3H10T_{\frac{1}{2}}$ cells were loaded to steady state with $^{45}Ca^{2+}$, and from time 0 onwards incubated in an unlabelled efflux medium containing 2 $\mu$M thapsigargin. The stores were challenged with Ins(1,4,5)$P_3$ using a protocol in which the Ins(1,4,5)$P_3$ concentration was gradually increased from 3.2 nM to 3.2 $\mu$M over a period of 6 min, i.e. in 60 steps each lasting 6 s. This procedure allows an accurate determination of the threshold for Ins(1,4,5)$P_3$ action [28]. This threshold was reached at lower Ins(1,4,5)$P_3$ concentrations in A7r5 cells [24 nM Ins(1,4,5)$P_3$] than in $C_3H10T_{\frac{1}{2}}$ cells [83 nM Ins(1,4,5)$P_3$]. This shift in threshold could reflect the activity of the major isoforms in these cell types, since Ins(1,4,5)$P_3$R-III was shown to have an approx. ten-fold lower affinity for Ins(1,4,5)$P_3$ than did Ins(1,4,5)$P_3$R-I [5].

## DISCUSSION

In our previous analysis [4] we have proposed the presence of an additional member of the Ins(1,4,5)$P_3$R family. This suggestion was based on the observation that in a number of mouse cell lines there was no indication of the presence of the type II, III or IV Ins(1,4,5)$P_3$Rs for which only limited sequence information was available [15]. In contrast, most of these cell lines expressed significant amounts of a mRNA that was very similar to, but not identical with, the published sequence of the type II and IV Ins(1,4,5)$P_3$R. We therefore tentatively designated this new mRNA as a fifth member of the Ins(1,4,5)$P_3$R family. It was remarkable, however, that the cell types of rat origin did not express this fifth isoform. It was even more remarkable that Ins(1,4,5)$P_3$R-III was not detected in the investigated mouse cell lines, whereas it was a major form in some of the rat cell lines. In the present study we have first screened a cDNA library constructed from $C_3H10T_{\frac{1}{2}}$-cell mRNA, in order to find a trace of the presumed isoform diversity. By screening with a PCR-amplified probe which was derived from a clone of the presumed type V Ins(1,4,5)$P_3$R from $C_3H10T_{\frac{1}{2}}$ cells, we indeed found a large number of positive clones, but all of them represented the same mRNA and there was no indication for the presence of the very related type II or type IV sequences. On the other hand, it was possible to amplify from $C_3H10T_{\frac{1}{2}}$ cell mRNA a type III-like Ins(1,4,5)$P_3$R using PCR primers, but again the sequence slightly deviated from the published one for mouse Ins(1,4,5)$P_3$R-III [15]. Table 2 is very relevant in resolving the apparent confusion with respect to the presence of different Ins(1,4,5)$P_3$R isoforms. It is evident that the $C_3H10T_{\frac{1}{2}}$ sequences detected in the present study show nearly the same identity with the rat analogues as was found for mouse and rat Ins(1,4,5)$P_3$R-I (about 94.5 %). We therefore assume that our sequences represent the mouse equivalents of the fully cloned rat sequences. This assumption is entirely confirmed by the observation that the PCR analysis based on the

sequences derived from the $C_3H10T_{\frac{1}{2}}$ cells yielded consistent expression patterns for these three Ins(1,4,5)$P_3$R isoforms in all samples, both from cultured cells and from animal tissues. We have no explanation for the sequence differences between the mouse Ins(1,4,5)$P_3$R sequences obtained in our study and the previously reported sequences of a type II, III and IV Ins(1,4,5)$P_3$R in mouse placenta [15]. It is very remarkable that mRNA corresponding to the latter sequences was never detected in any of the examined mouse tissues or cell lines. The ratio PCR method and the use of isoform-specific restriction-enzyme analysis should have revealed their presence if levels above background were expressed in these cells. The latter sequences published by Ross et al. [15], however, showed a significantly higher sequence identity with the equivalent rat Ins(1,4,5)$P_3$Rs (98–99%) than with the mouse Ins(1,4,5)$P_3$Rs found in our study (about 94%). In addition the sequence described for the type IV Ins(1,4,5)$P_3$R was only found in RBL-2H3 mast cells, which is a cell line of rat origin [4]. It is therefore conceivable that these sequences were erroneously described as mouse sequences, but that they rather represent rat or another very related species. It remains possible, however, that the differences reflect different mouse strains. Our assays were performed on cultured cells originating from several mouse strains ($BC_3H1$, $C_3H10T_{\frac{1}{2}}$, C2C12, Sol8 and L cells were from adult or embryonic $C_3H$ mice, neuro-2a cells were from strain A albino mouse and 3T3 cells from Swiss albino mouse), as well as on tissues from adult NMRI mouse, and all contained the same Ins(1,4,5)$P_3$R mRNAs.

The method described here is essentially the same as the ratio PCR method described in the previous study [4]. This method was developed for the determination of the relative levels of different highly homologous mRNAs in the same sample. The quantification is entirely based on the assumption that these very similar mRNAs will be amplified with the same efficiency if common primers are used and if the length of the amplification product is not too different. These conditions were fulfilled in the present study by using different primer pairs each of which could amplify two mRNAs with optimal efficiency. Although two such primer pairs are sufficient to calculate the expression levels of the three mRNAs, we have introduced a third primer pair which could serve as an additional control. Consistent ratios could be obtained from which the final expression pattern was derived. A similar method was described using primer pairs in the Ins(1,4,5)$P_3$-binding domain, which is also a region of very high homology [30]. There is generally a very good agreement of the data obtained here with literature data obtained with other methods such as RNA blot analysis, hybridization *in situ*, or immunoblotting, although in most cases the latter methods do not readily allow quantitative determinations. A notable exception is a recent analysis by quantitative immunoblotting [6] that showed very good general agreement with our data for a number of rat cell lines and tissues, suggesting that the mRNA expression is also relevant for protein levels of these isoforms. The latter study, however, also demonstrated a differential down-regulation of the three isoforms during activation of phosphoinositide hydrolysis. This constitutes at least one caveat for data obtained from mRNA expression.

In most studies Ins(1,4,5)$P_3$R-I was found to be ubiquitously expressed, but it is particularly predominant in the central nervous system [31,32] and in oocytes and eggs [16,24,25,33]. Ins(1,4,5)$P_3$R-II was reported to be less widely expressed and to be found particularly in some epithelia such as in the intralobular ducts of the salivary gland, epididymis, oviduct epithelium and renal proximal tubule [16], in the renal collecting duct [34] and in some renal cell lines [35]. In agreement with these findings, our sample from mouse kidney showed a very high expression of Ins(1,4,5)$P_3$R-II. High expression of this isoform was also described for the liver ([4–6,15] and the present study). In addition we have found very high expression of Ins(1,4,5)$P_3$R-II in cardiac and in skeletal muscle samples. Until now only the expression of the type I Ins(1,4,5)$P_3$R was reported in heart [36–38] and in fast-twitch and slow-twitch skeletal muscle [39]. Our present study indicated that there is a co-expression of the three isoforms and that Ins(1,4,5)$P_3$R-II is a major isoform in muscle cells. A similar expression pattern for rat heart was also found by immunoblotting [6]. Divergent findings were obtained for exocrine pancreas, where Ins(1,4,5)$P_3$R-II was also a major isoform ([4,6] and the present study), but in other reports a high expression of Ins(1,4,5)$P_3$R-III was found [12,16,40]. Several studies have shown a high expression of Ins(1,4,5)$P_3$R-III in cell types from endocrine pancreas [9,16] and in insulinoma cells [4,6,9]. The sample used in our study contained both endocrine and exocrine pancreas. Ins(1,4,5)$P_3$R-III was also reported to be highly expressed in the gastrointestinal tract, particularly in small-intestinal crypt and villous cells, and in gastric gland [5,9,12,15,16]. Testis ([5,6] and the present study), spleen [5] and thymus (the present study) were found to express significant levels of all three isoforms, including high levels of Ins(1,4,5)$P_3$R-III.

All cultured cell types expressed high levels of Ins(1,4,5)$P_3$R-III. This could indicate that there is a relation between cell proliferation and Ins(1,4,5)$P_3$R-III expression. The tissues rich in type III are also in most cases tissues with considerable cell turnover. Also some cultured cells derived from cell types that normally express Ins(1,4,5)$P_3$R-II, such as liver and kidney, express in addition high levels of Ins(1,4,5)$P_3$R-III. This was the case for WB, a clonal cell line from rat liver [41], MDCK [35,42] and $LLC\text{-}PK_1$ [35] renal cell lines. We found a similar phenomenon for the neuro-2a cells and for the muscle cell lines, where the expression pattern deviated from the tissue of origin with a very high expression of Ins(1,4,5)$P_3$R-III. In the neuro-2a cells, the induction of neurite formation resulted in a change in the expression pattern of the Ins(1,4,5)$P_3$R mRNAs. Ins(1,4,5)$P_3$R-I decreased in favour of a higher expression of Ins(1,4,5)$P_3$R-II, but Ins(1,4,5)$P_3$R-III remained the major isoform. The muscle cells shifted from a proliferating myoblast phenotype to myocytes [17], which in the case of C2C12 and Sol8 cells resulted in myotube formation for a fraction of the cells. As a result there was a clear tendency for a decrease in the relative level of type III expression and an increase in the proportion of the other isoforms, particularly type II. The muscle cell lines seem to change in the direction of the situation for adult skeletal muscle tissue, although this change occurs only to a limited extent.

Our data, showing that multiple Ins(1,4,5)$P_3$Rs are expressed in every cell type, are in agreement with other findings and support the view that these isoforms are probably functionally different and their expression correlates with the appearance of particular functions [5,6,35,43–45]. The changes in differentiating muscle cells as well as in the neuro-2a cells support this view. We have performed a functional assay on A7r5 and $C_3H10T_{\frac{1}{2}}$ cells, which are excellent model systems for measuring Ins(1,4,5)$P_3$-mediated $Ca^{2+}$ fluxes in permeabilized cell monolayers [4,26] and for which the expression patterns showed a marked difference both at the mRNA and at the protein level. The flux analysis on A7r5 and $C_3H10T_{\frac{1}{2}}$ cells revealed subtle differences in the release properties. This method, where cumulative doses of Ins(1,4,5)$P_3$ were given in small increments, allows one to obtain an accurate determination of the threshold for Ins(1,4,5)$P_3$ action. The threshold for Ins(1,4,5)$P_3$ was significantly higher for $C_3H10T_{\frac{1}{2}}$ cells. The observed difference between $C_3H10T_{\frac{1}{2}}$ cells and A7r5 cells may be due to dissimilar affinities of the major

expressed Ins(1,4,5)$P_3$R isoform in these cells, which is type III and type I respectively. In a study where the affinity of bacterial recombinant ligand-binding domains of these two isoforms was measured under identical experimental conditions, an approx. 10-fold difference was found between both isoforms [5]. On the other hand, Ins(1,4,5)$P_3$-mediated $Ca^{2+}$ release in astrocytes appeared to be more sensitive to Ins(1,4,5)$P_3$ than in Purkinje neurons [46], although the expression pattern of the Ins(1,4,5)$P_3$R indicated that astrocytes expressed type III and Purkinje cells type I [47]. The disparity in Ins(1,4,5)$P_3$ sensitivity may therefore equally well result from other modulators of Ins(1,4,5)$P_3$-mediated $Ca^{2+}$ release, such as phosphorylation status, ATP and $Ca^{2+}$, the action of which may depend on the isoform but also on the cellular context. The good agreement between expression pattern and function in our flux assay may be due to the fact that the effect of many intracellular modulators is no longer operative in the permeabilized cell system.

In summary, the present analysis yielded entirely consistent Ins(1,4,5)$P_3$R expression patterns in mouse cells, using sequence information for Ins(1,4,5)$P_3$R-I as well as for the mouse equivalents of rat Ins(1,4,5)$P_3$R-II and Ins(1,4,5)$P_3$R-III, which were partially cloned from $C_3H10T\frac{1}{2}$ cells. In contrast with previous reports [4,15], there is no evidence for the existence of other isoforms in the investigated mouse cells. The expression patterns revealed the simultaneous expression of different isoforms in the same cell type, which suggests some functional specialization. In this respect it was found that Ins(1,4,5)$P_3$R-I was the predominant isoform in brain, Ins(1,4,5)$P_3$R-II was highly expressed in some epithelial cell types as well as in muscle cells, whereas Ins(1,4,5)$P_3$R-III showed remarkably high expression in most of the cultured cells. The latter observation, as well as the shift from type III to type II during myoblast differentiation, could suggest a relation of the type III isoform with cell proliferation. In the particular case of A7r5 and $C_3H10T\frac{1}{2}$ cells, we found that the mRNA expression pattern correlated very well with the protein expression levels as well as with the functional properties of Ins(1,4,5)$P_3$-mediated $Ca^{2+}$ release in these cells.

We acknowledge the skilful assistance of Miss L. Bauwens, Mrs. M. Crabbé, Mrs. A. Florizoone, and Mrs. I. Willems. We are grateful to Dr. K. Mikoshiba (University of Tokyo, Japan) for sending us preprints of recent data. J.B.P. is Research Associate and I.S. is Research Assistant of the Foundation for Scientific Research (F.W.O.). This work was supported by the F.W.O. (Belgium).

## REFERENCES

1 Berridge, M. J. (1993) Nature (London) **361**, 315–325
2 McPherson, P. S. and Campbell, K. P. (1993) J. Biol. Chem. **268**, 13765–13768
3 Furuichi, T., Kohda, K., Miyawaki, A. and Mikoshiba, K. (1994) Curr. Opin. Neurobiol. **4**, 294–303
4 De Smedt, H., Missiaen, L., Parys, J. B., Bootman, M. D., Mertens, L., Van Den Bosch, L. and Casteels, R. (1994) J. Biol. Chem. **269**, 21691–21698
5 Newton, C. L., Mignery, G. A. and Südhof, T. C. (1994) J. Biol. Chem. **269**, 28613–28619
6 Wojcikiewicz, R. J. H. (1995) J. Biol. Chem. **270**, 11678–11683
7 Mignery, G. A., Newton, C. L., Archer, III, B. T. and Südhof, T. C. (1990) J. Biol. Chem. **265**, 12679–12684
8 Südhof, T. C., Newton, C. L., Archer, III, B. T., Ushkaryov, Y. A. and Mignery, C. A. (1991) EMBO J. **10**, 3199–3206
9 Blondel, O., Takeda, J., Janssen, H., Seino, S. and Bell, G. I. (1993) J. Biol. Chem. **268**, 11356–11363
10 Morgan, J. M., De Smedt, H. and Gillespie, J. I. (1996) Pflügers Arch. **431**, 697–705
11 Yamamoto-Hino, M., Sugiyama, T., Hikichi, K., Mattei, M. G., Hasegawa, K., Sekine, S., Sakurada, K., Miyawaki, A., Furuichi, T., Hasegawa, M. and Mikoshiba, K. (1994) Receptors Channels **2**, 9–22
12 Maranto, A. R. (1994) J. Biol. Chem. **269**, 1222–1230
13 Yamada, N., Makino, Y., Clark, R. A., Pearson, D. W., Mattel, M.-G., Guénet, J.-L., Ohama, E., Fujino, I., Miyawaki, A., Furuichi, T. and Mikoshiba, K. (1994) Biochem. J. **302**, 781–790
14 Harnick, D. E., Jayaraman, T., Go, L., Ma, Y., Mulieri, P. and Marks, A. R. (1995) J. Biol. Chem. **270**, 2833–2840
15 Ross, C. A., Danoff, S. K., Schell, M. J., Snyder, S. H. and Ullrich, A. (1992) Proc. Natl. Acad. Sci. U.S.A. **89**, 4265–4269
16 Fujino, I., Yamada, N., Miyawaki, A., Hasegawa, M., Furuichi, T. and Mikoshiba, K. (1995) Cell Tissue Res. **280**, 201–210
17 De Smedt, H., Parys, J. B., Himpens, B., Missiaen, L. and Borghgraef, R. (1991) Biochem. J. **273**, 219–224
18 Riboni, L., Prinetti, A., Bassi, R., Caminiti, A. and Tettamanti, G. (1995) J. Biol. Chem. **270**, 26868–26875
19 Chirgwin, J.-M., Przybyla, A. E., MacDonald, R. J. and Rutten, W. J. (1979) Biochemistry **18**, 5294–5299
20 Furuichi, T., Yoshikawa, S., Miyawaki, A., Wada, K., Maeda, N. and Mikoshiba, K. (1989) Nature (London) **342**, 32–38
21 Parys, J. B., De Smedt, H., Missiaen, L., Bootman, M. D., Sienaert, I. and Casteels, R. (1995) Cell Calcium **17**, 239–249
22 Lowry, O. H., Rosebrough, N. J., Farr, A. L. and Randall, R. J. (1951) J. Biol. Chem. **193**, 265–275
23 Laemmli, U. K. (1970) Nature (London) **227**, 680–685
24 Parys, J. B., Sernett, S. W., DeLisle, S., Snyder, P. M., Welsh, M. J. and Campbell, K. P. (1992) J. Biol. Chem. **267**, 18776–18782
25 Parys, J. B., McPherson, S. M., Mathews, L., Campbell, K. P. and Longo, F. (1994) Dev. Biol. **161**, 466–476
26 Missiaen, L., De Smedt, H., Droogmans, G. and Casteels, R. (1992) Nature (London) **357**, 599–602
27 Missiaen, L., De Smedt, H., Parys, J. B. and Casteels, R. (1994) J. Biol. Chem. **269**, 7238–7242
28 Missiaen, L., De Smedt, H., Parys, J. B., Sienaert, I., Vanlingen, S. and Casteels, R. (1996) J. Biol. Chem. **271**, 12287–12293
29 Parys, J. B., Missiaen, L., De Smedt, H. and Casteels, R. (1993) J. Biol. Chem. **268**, 25206–25212
30 Enyedi, P., Szabadkai, G., Horváth, A., Szilágyi, L., Gréf, L. and Spät, A. (1994) Endocrinology (Baltimore) **134**, 2354–2359
31 Furuichi, T., Shiota, C. and Mikoshiba, K. (1990) FEBS Lett. **267**, 85–88
32 Furuichi, T., Simon-Chazottes, D., Fujino, I., Yamada, N., Hasegawa, M., Miyawaki, A., Yoshikawa, S., Guénet, J.-L. and Mikoshiba, K. (1993) Receptors Channels **1**, 11–24
33 Kume, S., Muto, A., Aruga, J., Nakagawa, T., Michikawa, T., Furuichi, T., Nakade, S., Okano, H. and Mikoshiba, K. (1993) Cell **73**, 555–570
34 Yang, T., Terada, Y., Nonoguchi, H., Tomita, K. and Marumo, F. (1995) Am. J. Physiol. **268**, F1046–F1052
35 Monkawa, T., Miyawaki, A., Sugiyama, T., Yoneshima, H., Yamamoto-Hino, M., Furuichi, T., Saruta, T., Hasegawa, M. and Mikoshiba, K. (1995) J. Biol. Chem. **270**, 14700–14704
36 Gorza, L., Schiaffino, S. and Volpe, P. (1993) J. Cell Biol. **121**, 345–353
37 Kijima, Y., Saito, A., Jetton, T., Magnuson, M. and Fleischer, S. (1993) J. Biol. Chem. **268**, 3499–3506
38 Moschella, M. C. and Marks, A. R. (1993) J. Cell Biol. **120**, 1137–1146
39 Moschella, M. C., Watras, J., Jayaraman, T. and Marks, A. R. (1995) J. Muscle Res. Cell Motility **16**, 390–400
40 Nathanson, M. H., Fallon, M. B., Padfield, P. J. and Maranto, A. R. (1994) J. Biol. Chem. **269**, 4693–4696
41 Joseph, S. K., Lin, C., Pierson, S., Thomas, A. P. and Maranto, A. (1995) J. Biol. Chem. **270**, 23310–23316
42 Busch, K. T., Stuart, R. O., Li, S., Moura, L. A., Sharp, A. H., Ross, C. A. and Nigam, S. K. (1994) J. Biol. Chem. **269**, 23694–23699
43 Sugiyama, T. S., Yamamoto-Hino, M., Miyawaki, A., Furuichi, T., Mikoshiba, K. and Hasegawa, M. (1994) FEBS Lett. **349**, 191–196
44 Sugiyama, T., Furuya, A., Monkawa, T., Yamamoto-Hino, M., Satoh, S., Ohmori, K., Miyawaki, A., Hanai, N., Mikoshiba, K. and Hasegawa, M. (1994) FEBS Lett. **354**, 149–154
45 Li, M., Miyawaki, A., Yamamoto-Hino, M., Yasutomi, D., Furuichi, T., Hasegawa, M. and Mikoshiba, K. (1996) Biomed. Res. **17**, 45–51
46 Khodakhah, K. and Ogden, D. (1993) Proc. Natl. Acad. Sci. U.S.A. **90**, 4976–4980
47 Yamamoto-Hino, M., Miyawaki, A., Kawano, H., Sugiyama, T., Furuichi, T., Hasegawa, M. and Mikoshiba, K. (1995) NeuroReport **6**, 273–276

Received 16 September 1996/31 October 1996; accepted 1 November 1996